Journal of the Korean Physical Society, Vol. 67, No. 7, October 2015, pp. 1222∼1227

CdSe Nanowires Grown by Using Chemical Bath Deposition

H. Metin GUBUR*
Department of Physics, Mersin University, TR-33343 Yenisehir, Mersin, Turkey Advanced Technology Research & Application Center, Mersin University, TR-33343 Yenisehir, Mersin, Turkey

F. Septekin
Advanced Technology Research & Application Center, Mersin University, TR-33343 Yenisehir, Mersin, Turkey

S. Alpdogan
Department of Physics, Mersin University, TR-33343 Yenisehir, Mersin, Turkey

(Received 17 August 2015)

The Cadmium-selenide (CdSe) nanowire thin films were prepared on glass substrates by using chemical bath deposition (CBD) at 70 °C. Cadmium sulfate and sodium selenosulphate were used as Cd^{2+} and Se^{2-} ion sources, respectively. The CdSe nanowire film was annealed in an air atmosphere at 573 K for 1 hour. X-ray diffraction (XRD) results showed that the nanowire films as-deposited and annealed had mixed cubic and hexagonal phase. Scanning electron microscopy (SEM) indicated that the CdSe nanowires had lengths ranging from 642 nm to 2.5 μm and diameters ranging from 46 nm to 211 nm. The optical properties of the as-deposited and the annealed nanowire films, an investigated by recording the transmission spectra by using an UV-visible spectrophotometer revealed that the energy band gap decreased (from 1.78 eV to 1.50 eV) upon annealing. The conductivity measurements made by using four-probe methods for both the annealed and the as-deposited films showed that the resistivity, conductivity and activation energy changed upon annealing.

PACS numbers: 73.20.-r, 73.61.Ga, 73.61.-r
Keywords: CdSe, Nanowire, CBD, Structural, optical and electrical properties
DOI: 10.3938/jkps.67.1222

I. INTRODUCTION

Nanoscaled semiconductors, which are used in electronic, optical, photovoltaic and biological devices, have been studied by many researchers for several years. Also, recently, one-dimensional semiconductor nanowires were widely examined for their optical and electronic properties due to their convenient length and structure [1–10]. Thanks to these features, nanowires are easily used in nanostructure optical and electronic devices such as solar cells [11–16], lasers [17–20], transistors [21–23], light-emitting diodes [24–27] and photodetectors [28,29]. For example, cadmium selenide (CdSe) has a direct band gap 1.70 eV, an important nanostructure semiconductor II-VI group compounds in the periodic table. CdSe nanowires are of great importance because they have a blue-shift in the photoluminescence and very settable luminescence properties corresponding to the quantum confinement effect [30]. Several research groups have grown Nanocrystalline CdSe by using many physical and chemical methods: molecular beam epitaxy [31], electrodeposition [9,32], spray pyrolysis [33], chemical vapor deposition [34, 35], metal organic chemical vapor deposition [36], successive ionic layer adsorption and reaction method (SILAR) [37], and chemical bath deposition (CBD) [38–40]. Among these techniques, the chemical bath deposition technique is known to be simple and inexpensive because the equipment used for this technique is easily available in many research laboratories. However, parameters such as the solutions concentration, the solution's pH and the storage temperature are very important in terms of a film quality during the fabrication of CdSe. In this regard, quality semiconductor nanowire thin films with wide surfaces can be produced by using the chemical bath deposition because that method provides control of those parameters. In the present research, the structural, optical and electrical properties of CdSe nanowire thin films grown by using chemical bath deposition at 70 °C were studied.

*E-mail: hulmetin@gmail.com; Fax: +90-324-361-0046

II. EXPERIMENTS

The CdSe nanowire thin films were deposited on glass substrates by using chemical bath deposition at 70 °C. The chemical bath prepared for the deposition of the CdSe nanowire thin films contained sodium sulfite, sodium selenosulfate, cadmium nitrate, triethannolamine (TEA), ammonia solution, and deionized water. The experimental details (substrate cleaning and the method of deposition) are discussed in our previous publication [40]. In this study, the stock solution and the thickness were different from there in our previous studies, and the solution for this research was prepared as 0.225 M. Also, the thickness of the films was found to be 1.20 μm. We fabricated two films: the as-deposited film and the annealed film in air at 573 K.

The structural studies were carried out by using a Bruker AXS Advance D8 diffractometer with the help of EVA and Win index software in the range of diffraction angles $20° \leq 2\theta \leq 70°$ in steps of 0.02° at 40 kV and 30 mA with CuK 1 radiation ($\lambda = 1.5406$ Å). The surface morphology of the CdSe nanowires was scanned at various magnifications by using a Zeiss-Supra 55 scanning electron microscope equipped with an energy dispersive X-ray (EDX) spectrometer and a computer-controlled image analyzer. The optical transmission spectra and the thicknesses of the CdSe nanowires were recorded by using Shimadzu UV-1700 and Analytic Jena-Specord 210 Plus UV-visible spectrophotometer in the wavelength range of 190 − 1100 nm at room temperature. The four-point probe technique was used to measure the temperature dependence of the electrical resistivity of the films. The particulars of the experimental setup are given Ref. [40].

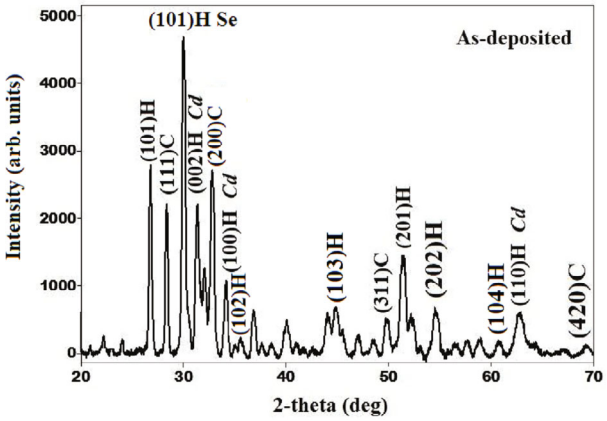

Fig. 1. X-ray diffraction pattern of the as-deposited CdSe nanowires.

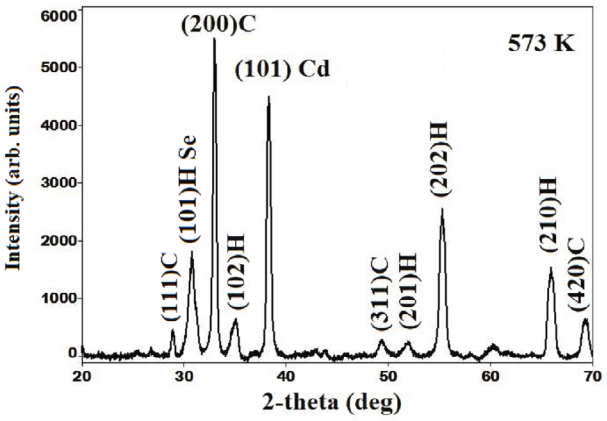

Fig. 2. X-ray diffraction pattern of the CdSe nanowires annealed at 573 K in air.

III. RESULTS AND DISCUSSION

1. Structural Properties

The X-ray diffraction (XRD) patterns of the as-deposited CdSe nanowire and of the CdSe nanowire annealed at 573 K are shown in Fig. 1 and Fig. 2, respectively. By using the standard phase of the "d" for the CdSe nanowires, which are given by cubic (C) (PDF Card No: 077-7287, PDF Card No: 088-2346) and hexagonal (H) (PDF Card No: 075-5680, PDF Card No: 002-0330, PDF Card No: 001-1175, PDF Card No: 005-0674), the plane indices of the observed "d" are obtained. The standard "d" values are in good agreement with the observed "d" values for the cubic and hexagonal structure of CdSe. The nanowire films as-deposited and annealed were found to have mixed cubic and hexagonal phase. The diffraction peaks observed in films as-deposited and annealed at 573 K one significantly different; for instance, while the intensity of the reflection peaks of the Cd crystal increased with increasing annealing temperature, the intensity of the reflection peaks of the Se crystal was decreased with annealing temperature. Therefore, we can say that the amount of selenium decreased with increasing annealing temperature.

The crystallite size of the CdSe nanowires was calculated from the full width at half maximum (FWHM) of the (200) peak for the cubic phase by using the Debye-Scherrer formula [40]. The dislocation densities ($\delta = n/D_{hkl}^2$), the number of crystallites /unit area ($N = d/D_{hkl}^3$), and the strains ($\varepsilon = \beta \cos\theta/4$) in the CdSe nanowire films were obtained by using the relevant equations and are given in Table 1. While the crystallite size of the nanowire films increased with increasing annealing temperature, the dislocation densities, the number of crystallites/unit area and the strains decreased.

The scanning electron microscopy (SEM) images of the as-deposited and the annealed CdSe nanowires are shown in Fig. 3. The SEM images of the as-deposited and the annealed CdSe nanowires were examined at low and high magnifications. At the low magnifications, the top surface images and at the high magnifications,

Table 1. FWHM, crystallite size, dislocation density, number of crystallites/unit area, and strain for the as-deposited and the annealed CdSe nanowires.

Annealing temperature (K)	FWHM β (rad)	Crystallites size (nm)	Dislocation density (10^{15} lines m^{-2})	Number of crystallites/unit area (10^{17} m^{-2})	Strain (10^{-3})
As-deposited	0.0084	17.26	3.35	2.33	2.016
573	0.0062	23.46	1.82	0.93	1.476

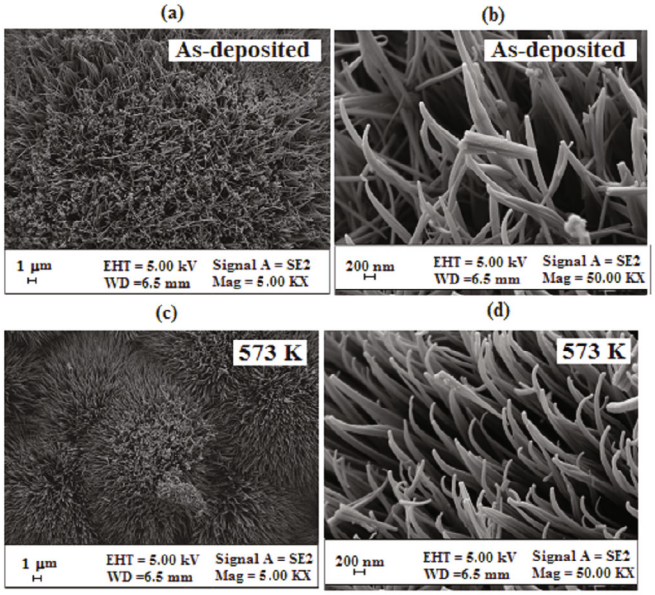

Fig. 3. SEM images of the as-deposited and the annealed CdSe nanowires: (a) and (c) 5.00 KX magnification of the top surfaces and (b) and (d) 50.00 KX magnification of the cross-sectional surfaces.

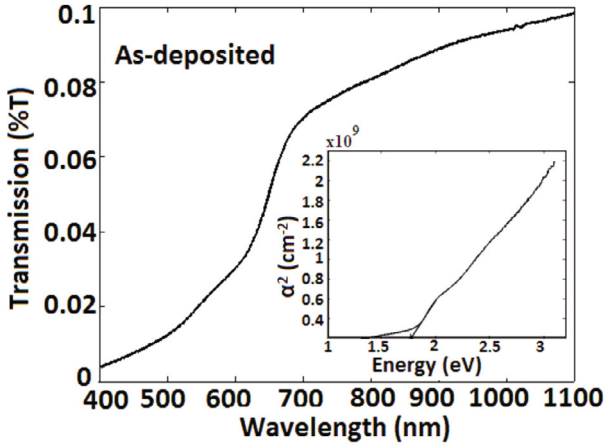

Fig. 4. Optical transmission spectrum of the as-deposited CdSe nanowires. The α^2 versus photon energy curve is given inset.

the cross-sectional surface images of the as-deposited and the CdSe thin films annealed in air at 573 K are shown in Figs. 3(a)−(c) and Figs. 3(b)−(d), respectively. The surface morphology of the CdSe was found to be CdSe nanowires. The top surface images of the CdSe nanowires in Figs 3(a)−(c) were well-covered, uniform and homogeneous, without cracks and voids on the surface of the substrate. Figures 3(b)−(d), cross-sectional surface images, showed that the nanowires had elongated rod shapes and a uniform diameter. The CdSe nanowires can also be seen to have lengths ranging from 642 nm to 2.5 μm and diameters ranging from 46 nm to 211 nm. When the annealing temperature was increased, the range of diameters for the CdSe nanowires; for example, while the diameters of the as-deposited CdSe nanowires ranged from 82 nm to 211 nm, those of the annealed CdSe nanowires ranged from 46 nm to 142 nm. Also, Figs. 3(b)−(d) shown that the structure of the annealed CdSe nanowires was more regular than that of the as-deposited CdSe nanowires. Further, CdSe nanowires are known to have tapered ends, so they are very efficient at capturing light. Additionally, as the number of CdSe nanowires per surface area is large than it is far other structures, these CdSe nanowires can significantly contribute to the surface energy.

2. Optical Properties

Figures 4 and 5 show the transmission spectra (range 400 nm to 1100 nm) of the as-deposited and the annealed CdSe nanowires. The equations used for the calculation of the thicknesses and the absorption coefficients (α) of the films are discussed in our previous publication [40]. The CdSe nanowires had an absorption edge at approximately 700 nm, which is attributed to the band gap of CdSe, and the CdSe nanowires have a direct optical band gap. The α^2 versus photon energy curves for these films are given as insets in Figs. 4 and 5. The optical band gap energy (E_g) is known to be the value of the energy for $\alpha^2 = 0$. The optical band gap energies of the as-deposited and the annealed CdSe nanowires decreased from 1.77 eV to 1.50 eV with increasing annealing temperature. The E_g of the as-deposited film (1.77 eV) is very close to that of bulk CdSe (1.75 eV). This result shows a blue

Table 2. Activation energies and resistivities of the as-deposited and the annealed CdSe nanowires.

Annealing temperature (K)	Activation energy E_a (eV) LT	Activation energy E_a (eV) HT	Resistivity ρ (Ω-cm) 320 K	Resistivity ρ (Ω-cm) 623 K
As-deposited	0.22	0.55	2.92×10^7	1.37×10^5
573	0.17	0.52	3.98×10^7	1.40×10^4

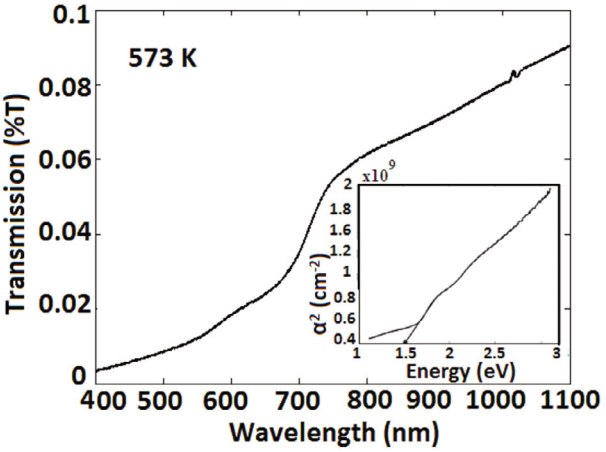

Fig. 5. Optical transmission spectrum of CdSe nanowires annealed at 573 K in air. The α^2 versus photon energy curve is given inset.

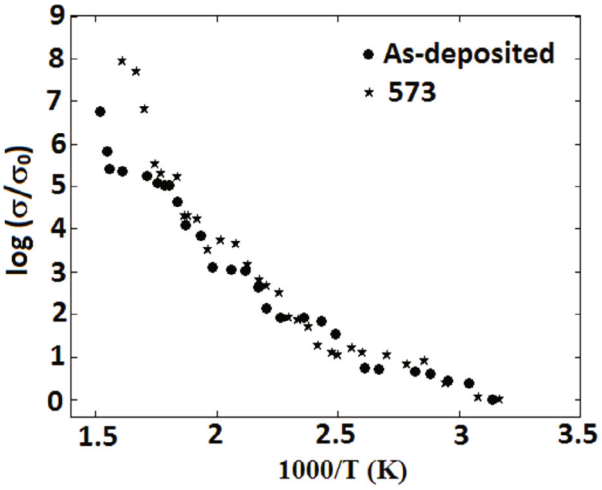

Fig. 6. Temperature dependences of the electrical conductivity for the as-deposited and the annealed CdSe nanowires.

shift from the energy band gap of 1.75 because of the quantum confinement effect in nanostructure materials [41].

3. Electrical Properties

The transport phenomenon can be explained by the electrical conductivity, and the electrical properties of nanocrystalline semiconductors are considerable for the conduction mechanism [42–44]. Nanocrystalline materials have large grain boundaries and small grain sizes, so the electronic states around the Fermi levels are localized. The conduction mechanism appears to be due to a bouncing of carriers between occupied and empty localized states which is based on the position of the Fermi level and the state density when the electronic states are localized [44–46]. The conductivity measurement shows that the thin films have an electrical resistivity on the order of 10^6 Ω-cm at room temperature.

Variations in the electrical conductivity of these films with temperature were determined by using the four-point probe technique. The details of this technique are discussed in our previous publication [40]. In Fig. 6, the temperature-dependent conductivity results for the films are given. The figure shows that two distinct conductivity curve shapes exist. As discussed in our previous publication [40], the conductivity of the films increases exponentially with increasing temperature, which shows a typical semiconductor behavior.

The activation energy of the CdSe nanowires was determined by using the relation $\sigma = \sigma_0 \exp(-E_a/k_B T)$, where σ is the conductivity of the films, σ_0 is the pre-exponential factor, T is the temperature, k_B is the Boltzmann constant and E_a is the activation energy [39]. In two different temperature regions, a high-temperature region (HT) (450 K $\leq T \leq$ 650 K) and a low temperature region (LT) (300 K $\leq T \leq$ 450 K), the activation energy values for both films were calculated. The activation energy decreased with increasing annealing temperature in the low- and high-temperature regions, as given in Table 2. These results indicate that less energy is required for the annealed films to begin an electrical transport mechanism than is required for the as-deposited films.

The results in Fig. 6 are interesting in that the annealed CdSe nanowire demonstrates semiconducting features earlier than the as-deposited CdSe nanowire. Thus, the annealed CdSe nanowire is a good semiconductor for use in semiconducting devices.

IV. CONCLUSION

In this study, CdSe nanowire thin films were prepared by using CBD at 70 °C. The structural measurements through XRD analysis demonstrated that the texture of the as-deposited and the annealed CdSe nanowire thin films had mixed cubic and hexagonal phases. The crystallites grew with increasing annealing temperature. Accordingly, the dislocation densities due to defects in the crystal, the number of crystallites/unit area, and the strains decreased. By investigating the SEM images, we found that the semiconductor CdSe nanowire thin films displayed the nanowire structures and that the CdSe nanowire thin films had lengths ranging from 642 nm to 2.5 μm and diameters ranging from 46 nm to 142 nm. The electrical properties of the CdSe nanowire thin films were presented, and the annealed CdSe nanowire was found to have a lower activation energy and to show a better thermal conduction mechanism at greater temperature than the as-deposited CdSe nanowire. Finally, considering all of these results, we can conclude that the CdSe nanowire thin films have good electrical conductivity, as well as good optical and crystal quality; therefore, the CdSe nanowire thin films can be used for electronic and solar-cell applications.

ACKNOWLEDGMENTS

This research was supported by the Mersin University Scientific Research Unit (contract nos.: BAP-FEF FB (HM) 2004-3 and BAP-FEF FB (FS) 2014-2 YL). The authors would like to thank the University of Mersin.

REFERENCES

[1] C. M. Lieber and Z. L. Wang, MRS Bull. **32**, 99 (2007).
[2] M. Law, J. Goldberger and P. D. Yang, Annu. Rev. Mater. Res. **34**, 83 (2004).
[3] W. Lu and C. M. Lieber, Nat. Mater. **6**, 841 (2007).
[4] A. L. Schmitt, J. M. Higgins, J. R. Szczech and S. Jin, J. Mater. Chem. **20**, 223 (2010).
[5] R. Yan, D. Gargas and P. Yang, Nat. Photonics **3**, 569 (2009).
[6] A. I. Hochbaum and P. Yang, Chem. Rev. **110**, 527 (2009).
[7] B. Tian, T. J. Kempa and C. M. Lieber, Chem. Soc. Rev. **38**, 16 (2009).
[8] H. Wu, F. Meng, S. Jin and G. Zheng, ACS nano. **6**, 4461 (2012).
[9] M. Kumari, R. Pallavi and R. P. Chauhan, Nucl. Instr. Meth. in Phys. Res. A. **753**, 116 (2014).
[10] D. M. Cardamone and G. Kirczenow, Nano Lett. **10**, 1158 (2010).
[11] W. U. Huynh, J. J. Dittmer and A. P. Alivisatos, Science **295**, 2425 (2002).
[12] Y. H. Yu, P. V. Kamat and M. A. Kuno, Adv. Funct. Mater. **20**, 1464 (2010).
[13] A. Kongkanand, K. Tvrdy, K. Takechi, M. Kuno and P. V. Kamat, J. Am. Chem. Soc. **130**, 4007 (2008).
[14] G. M. Wang, X. Y. Yang, F. Qian, J. Z. Zhang and Y. Li, Nano Lett. **10**, 1088 (2010).
[15] W. T. Sun, Y. Yu, H. Y. Pan, X. F. Gao, Q. Chen and L. M. Peng, J. Am. Chem. Soc. **130**, 1124 (2008).
[16] I. Gur , N. A. Fromer, M. L. Geier and A. P. Alivisatos, Science **310**, 462 (2005).
[17] A. Khandelwal, D. Jena, J. W. Grebinski, K. L. Hull and M. K. Kuno, J. Elect. Mater. **35**, 170 (2006).
[18] A. Pan, W. Zhou, E. S. P. Leong, R. Liu, A. H. Chin, B. Zou and C. Z. Ning, Nano Lett. **9**, 784 (2009).
[19] B. Piccione, L. K. van Vugt and R. Agarwal, Nano Lett. **10**, 2251 (2010).
[20] L. K. van Vugt, B. Piccione, C. Cho, C. Aspetti, A. D. Wirshba and R. Agarwal, J. Phys. Chem. A **115**, 3827 (2011).
[21] R. M. Ma, L. Dai, H. B. Huo, W. J. Xu and G. G. Oin, Nano Lett. **7**, 3300 (2007).
[22] Y. Zhang, Y. Tang, K. Lee and M. Ouyang, Nano Lett. **9**, 437 (2008).
[23] J. Debaets, J. Vanfl eteren I. Derycke, J. Doutreloigne, A. Vancalster and P. Devisschere, IEEE Trans. Electron. Dev. **37**, 636 (1990).
[24] S. C. Erwin, L. J. Zu, M. I. Haftel, A. L. Efros, T. A. Kennedy and D. J. Norris, Nature **436**, 91 (2005).
[25] Y. Huang, X. F. Duan and C. M. Lieber, Nanophotonics Small **1**, 142 (2005).
[26] C. H. Cho, C. O. Aspetti, M. E. Turk, J. M. Kikkawa, S. W. Nam and R. Agarwal, Nat. Mater. **10**, 669 (2011).
[27] M. Achermann, M. A. Petruska, S. Kos, D. L. Smith, D. D. Koleske and V. I. Klimov, Nature **429**, 642 (2004).
[28] S. H. Kang, H. H. Huh, K. C. Son, C. S. Lee, K. H. Kim, C. Huh and E. T. Kim, Physica Status Solidi B **246**, 889 (2009).
[29] Q. Yang, X. Guo, W. H. Wang, Y. Zhang, S. Xu, D. H. Lien and Z. L. Wang, ACS Nano **4**, 6285 (2010).
[30] Y. Yan, Z-M Liao, Y-Q Bie, H-C Wu, Y-B Zhou, X-W Fu and D-P Yu, Appl. Phys. Lett. **99**, 103103 (2011).
[31] N. Samarth, H. Luo, J. K. Furdyna, S. B. Qadri, Y. R. Lee, A. K. Ramdas Appl. Phys. Lett. N. Otsuka, Appl. Phys. Lett. **2680**, 54 (1989).
[32] K. R. Murali, V. Subramanian, N. Rangarajan, A. S. Lakshmanan and S. K. Rangarajan, J. Electroanal. Chem. **95**, 368 (1994).
[33] T. Elango, S. Subramanian and K. R. Murali, Surf. Coat. Technol. **8**, 123 (2003).
[34] R. Venugopal, P. I. Lin, C. C. Liu and Y. T. Chen, J. Am. Chem. Soc. **127**, 11262 (2005).
[35] Y. Du and G. Li, Physica E: Low-dimen. Syst. and Nanostruc. **43**, 994 (2011).
[36] H. M. Pathan, B. R. Sankpal, J. D. Desai and C. D. Lokhande, J. Mater. Chem. Phys. **78**, 11 (2003).
[37] C. D. Lokhande, B. R. Sankapal, S. D. Sartale, H. M. Pathan, M. Giersig and V. Ganesan, Appl. Surf. Sci. **413**, 182 (2001).
[38] R. B. Kale and C. D. Lokande, Semicond. Sci. Techol. **1**, 20 (2005).
[39] G. Hodes, A. Albu-Yaron, F. Decker and P. Motisuke, Phys. Rev. B **4215**, 36 (1987).
[40] S. Erat, H. Metin and M. Ari, Mater. Chem. Phys. **111**,

114 (2008).
[41] L. Zuala, R. Madaka and P. Agarwal, *Conference Papers in Science* (Hindawi Publishing Corporation, Bhubaneswar, 2013), Vol. 2013.
[42] S. Banerjee, S. Nozaki and H. Morisaki, J. Appl. Phys. **91**, 4307 (2002).
[43] S. K. Mandal, S. Chaudhuri and A. K. Pal, Nanostruct. Mater. **10**, 607 (1998).
[44] R. K. Joshi and H. K. Sehgal, Physica E **23**, 168 (2004).
[45] N. F. Mott and E. A. Davis, *Electronic Processes in Non-Crystalline Materials*, 2nd Edition (Oxford University Press, New York, 1979).
[46] M. S. Hossain, R. Islam and K. A. Khan, Renew. Energy **33**, 642 (2008).